Composite twin dark matter

John Terning,[*] Christopher B. Verhaaren,[†] and Kyle Zora[‡]

Department of Physics, University of California Davis, One Shields Avenue, Davis, California 95616, USA

We consider fraternal twin Higgs models where the twin bottom quark, b', is much heavier than the twin confinement scale. In this limit aspects of quark bound states, like the mass and binding energy, can be accurately calculated. We show that in this regime, dark matter can be primarily made of twin baryons containing $b'b'b'$ or, when twin hypercharge is gauged, twin atoms, composed of a baryon bound to a twin τ' lepton. We find that there are significant regions of parameter space which are allowed by current constraints but within the realm of detection in the near future. The case with twin atoms can alleviate the tension between dark matter properties inferred from dwarf galaxies and clusters.

I. INTRODUCTION

One of the most compelling motivations to search for new particles and interactions beyond the standard model (SM) is the so-called dark matter (DM) that makes up 80% of the matter density of the Universe. The indirect evidence for DM is overwhelming [1,2] but neither the mechanism for producing the inferred density of DM particles nor its mass or nongravitational interactions have been experimentally identified. The paradigm of asymmetric dark matter (ADM) [3] is motivated by the observation $\Omega_{\rm DM} \simeq 5\Omega_{\rm B}$, where $\Omega_{\rm DM}$ and $\Omega_{\rm B}$ are the DM and baryonic mass densities respectively. If matter/antimatter asymmetries in both the visible and dark sectors have a common origin, the similarity in their mass densities is natural, rather than a miraculous conspiracy between two *a priori* independent processes. In particular, we have

$$\frac{\Omega_{\rm DM}}{\Omega_{\rm B}} = \frac{\eta_{\rm DM}}{\eta_{\rm B}} \frac{m_{\rm DM}}{m_N}, \tag{1.1}$$

where $\eta_{\rm DM}$ ($\eta_{\rm B}$) sets the dark matter (baryon) asymmetry and m_N is the nucleon mass. Clearly, ADM is even more appealing in models where there is some symmetry between the dark and visible sectors, as in mirror world scenarios [4–6], which can ensure $\eta_{\rm DM} \sim \eta_{\rm B}$ and $m_{\rm DM} \sim m_N$.

[*]jterning@gmail.com
[†]cbverhaaren@ucdavis.edu
[‡]kezora@ucdavis.edu

Explaining the hierarchy between the weak scale and the higher scales associated with modifications of the SM, including the Planck scale, has long guided explorations beyond the SM. Within the variety of possibilities that have been considered, the paradigm of neutral naturalness encapsulates those frameworks which explain the little hierarchy, between the weak scale and a few TeV, through a new symmetry, but whose partner quarks do not carry SM color [7–18]. The first and most studied realization of this idea is the twin Higgs [7] scenario. It remains a future target of collider tests [19–31] and may also have connections to neutrinos [32] and flavor [33,34]. In addition, the twin Higgs is a simple, concrete framework for thinking about dark matter sectors with a rich variety of particles and interactions.

In twin Higgs constructions, the SM particle content is doubled, making a visible sector and a twin sector, which are related to each other by a discrete Z_2 symmetry. This means that the twin sector has the same gauge structure of the SM, but the gauge groups are distinct, so that the fields of one sector are gauge singlets of the other. In addition, the scalar potential is approximately invariant under an $SU(4)$ global symmetry [7]. When this symmetry is spontaneously broken by a vacuum expectation value (VEV) f down to $SU(3)$, seven pseudo-Nambu-Goldstone bosons result. Six are eaten by the $SU(2)$ gauge symmetries in either sector, leaving one physical Higgs boson. To satisfy experimental bounds on the couplings of the Higgs to SM fields, the discrete symmetry must be softly broken, such that the VEV in the SM sector $v = 246$ GeV is a few times smaller than f, $f/v \gtrsim 3$ [19]. The larger value of f leads to masses in the twin sector being raised beyond their SM counterparts

$$m_{\rm Twin} = \frac{f}{v} m_{\rm SM}. \tag{1.2}$$

If the ratio f/v is taken to be too large then the twin top-quark mass $m_{t'}$ becomes much heavier than the SM top quark, signaling a fine-tuning; for instance if $m_{t'} = 1$ TeV the theory is tuned to about 10% [19].

This mirror twin Higgs construction includes many new light states in the hidden sector. This seems at odds with cosmological measurements of the number of light relativistic species, in particular measurements of the cosmic microwave background (CMB) constrain $\Delta N_{\text{eff}} \lesssim 0.3$ at 95% confidence [35]. It has been shown that such cosmological tensions can be overcome [36–39] while continued analysis of cosmological data may reveal signatures of a twinlike structure [40–44]. Models of baryogenesis [45] as well as dark matter [46–51] have also been explored.

A simple way to relieve tension with ΔN_{eff} is to remove the light degrees of freedom (d.o.f.) from the twin sector. In the fraternal twin Higgs model [52] only the third generation of quarks and leptons are twinned.[1] This construction strives for minimal constraints from naturalness on the twin sector. Therefore, only the twin top quark t' needs to be a nearly exact twin, that is with the same Yukawa coupling to the Higgs. Other twin fields like the twin bottom quark, b', and twin tau, τ', can differ significantly from the mirror model expectation, as long as their Yukawas do not become close to top Yukawa size. Similarly, the twin strong coupling α'_s may not be exactly equal to the SM value at the cutoff of a few TeV. If it is too different, more than a few tens of percent, then the two-loop running of the top Yukawa diverges from the SM value, spoiling the cancellation of quadratic divergences. Of course, the different particle content at low energies means the twin QCD scale $\Lambda_{\text{QCD}'}$ can be considerably larger than the SM confining scale, often taking values of a few GeV. However, if the twin coupling is smaller than the SM value at the cutoff, confinement scales of a few hundred MeV can result while preserving naturalness.

This fraternal construction has been previously explored as an interesting candidate for ADM [48], but only in the regime where the b' mass is comparable or smaller than $\Lambda_{\text{QCD}'}$.[2] In the $m_{b'} \ll \Lambda_{\text{QCD}'}$ limit it is easy to estimate the mass of the stable baryon composed of twin bottom quarks leading to a robust analysis of the proposed dark sector, with or without gauging twin hypercharge. Here we explore the opposite regime where $m_{b'} \gg \Lambda_{\text{QCD}'}$. In this case the physics of the composite baryon is simpler; it can be understood using nonrelativistic quantum mechanics. However, it requires slightly more effort than the previous analysis to obtain an accurate mass estimate. In the next section we review the calculation of the baryon mass, and

then turn in Sec. III to the constraints on these baryons as an ADM candidate. In Sec. IV we consider the case that the twin hypercharge is gauged so that neutral twin atoms may form out of the twin baryon and the twin τ', which provides another interesting DM candidate. There we also comment on a possible resolution of the tension between dark matter self-interaction cross sections inferred from dwarf galaxies and the bullet cluster [54,55].

II. BARYON MASSES

In the heavy b' regime, $m_{b'} \gg \Lambda_{\text{QCD}'}$, we can treat the QCD$'$ coupling, $\alpha'_s = g_3'^2/(4\pi)$, as perturbative at scales of the size of the bound states. The lightest color neutral baryon, the analog of the spin $3/2$ Δ baryon, is then simply a Coulombic bound state of three identical heavy quarks, as long as the Bohr radius $\sim 1/(\alpha'_s m_{b'})$ is much smaller than the confinement length $\sim 1/\Lambda_{\text{QCD}'}$. We can then calculate approximate Δ' masses using a nonrelativistic Hamiltonian:

$$H = \sum_{i=1}^{3} \frac{\mathbf{p}_i^2}{2m_{b'}} - \frac{\mathbf{P}_{\text{CM}}^2}{2M} + \left(\frac{1}{9}\alpha' - \frac{2}{3}\alpha'_s\right) \sum_{i>j}^{3} \frac{1}{r_{ij}}, \quad (2.1)$$

where $\mathbf{P}_{\text{CM}}$ is the momentum of the center of mass, M is the total mass, α' is the coupling for twin QED, and $r_{ij} = |\mathbf{r}_i - \mathbf{r}_j|$ is the distance between the ith and jth quarks. The factor of $\frac{2}{3}$ arises from the Casimir of twin color generators $T^a T^a$ evaluated in the color singlet state. The baryon ground state can be roughly approximated by the wave function

$$\Psi(\mathbf{r}_1, \mathbf{r}_2, \mathbf{r}_3) = 8a^{9/2} \exp\left[-a(r_1 + r_2 + r_3)\right], \quad (2.2)$$

where a is a variational parameter. Using values $\alpha' = 1/137$ and $\alpha'_s = 0.15$, the variational binding energy is $E \approx -0.00865 m_{b'}$, so the baryon mass is about three times the mass of its heavy constituent quarks, as expected.

A more precise solution is obtained by using the stochastic variational method [56]. We use a correlated Gaussian (CG) basis

$$\phi(\mathbf{r}_1, \mathbf{r}_2, \mathbf{r}_3) = \exp\left(-\frac{1}{2}\sum_{i,j=1}^{2} A_{ij}\mathbf{x}_i \cdot \mathbf{x}_j\right), \quad (2.3)$$

where A is a positive definite matrix and the $\mathbf{x}_i$ are the Jacobi coordinates of the three-quark system. In particular,

$$\mathbf{x} = \mathbf{U}\mathbf{r}, \quad (2.4)$$

with

---

[1]The vectorlike twin Higgs [53] model provides vectorlike masses to the third generation quarks, removing the need for twin leptons to cancel gauge anomalies.

[2]In [49] the ADM construction is studied in the mirror twin Higgs model.

$$\mathbf{U} = \begin{pmatrix} 1 & -1 & 0 \\ 1/2 & 1/2 & -1 \\ 1/3 & 1/3 & 1/3 \end{pmatrix}. \tag{2.5}$$

Using Jacobi coordinates eliminates our need for a center of mass coordinate, which speeds up the calculation.

Since the three-quark color singlet is antisymmetric, and the complete three-quark wave function must be antisymmetric overall, we symmetrize the spatial wave function with

$$S = \frac{1}{\sqrt{3!}} \sum_n \mathbf{P_n}, \tag{2.6}$$

where the $\mathbf{P_n}$ are permutation elements of the symmetric group $\mathbf{S}_3$. This operator commutes with the Hamiltonian and has the property

$$S^\dagger S = \sqrt{3!}S. \tag{2.7}$$

We find a basis set, by first generating a set of random, positive definite matrices A and select the one which minimizes the binding energy. Additional matrices are added to the basis set when doing so reduces the binding energy by at least a specified amount. The energy is then calculated using the basis set of wave functions $|\phi_i\rangle$ to produce a variational wave function

$$|\Phi\rangle = \sum_i c_i |\phi_i\rangle. \tag{2.8}$$

We then solve the generalized eigenvalue problem for the vector c_i,

$$\mathcal{H}\mathbf{c} = E\mathcal{N}\mathbf{c}, \tag{2.9}$$

with $\mathcal{H}$ given by

$$\mathcal{H}_{ij} = \langle\phi_i|S^\dagger HS|\phi_j\rangle = \langle\phi_i|HS^\dagger S|\phi_j\rangle = \sqrt{3!}\langle\phi_i|HS|\phi_j\rangle, \tag{2.10}$$

and $\mathcal{N}$ defined to be

$$\mathcal{N}_{ij} = \langle\phi_i|S^\dagger S|\phi_j\rangle = \sqrt{3!}\langle\phi_i|S|\phi_j\rangle. \tag{2.11}$$

This yields the coefficients c_i that minimize the energy.

The resulting binding energy, using a basis of 29 wave functions, is

$$E_b \approx -0.475m_{b'}\left(\alpha_s'^2 - \frac{\alpha'\alpha_s'}{3} + \frac{\alpha'^2}{36}\right). \tag{2.12}$$

For comparison, with $\alpha' = 1/137$ and $\alpha_s' = 0.15$, we find a binding energy of $E \approx -0.0105m_{b'}$, which is 20% deeper than the naive estimate. The mass of the Δ' baryon is

$$m_{\Delta'} = 3m_{b'} + E_b \approx m_{b'}\left[3 - 0.475\left(\alpha_s'^2 - \frac{\alpha'\alpha_s'}{3} + \frac{\alpha'^2}{36}\right)\right]. \tag{2.13}$$

Here the running couplings should be evaluated at the scale of typical momentum transfer within the baryon, which is defined by

$$\mu \equiv \alpha_s'(\mu)m_{b'}. \tag{2.14}$$

This calculation of the binding energy assumed a Coulombic potential, but corrections from the confinement potential are of order $\Lambda_{\text{QCD}'}^2/\mu^2$. The full potential may be parametrized as

$$V_{\text{Total}} = V_{\text{Cou}} + V_{\text{Conf}} = \frac{2}{3}\frac{\alpha_s'}{r} + c\Lambda_{\text{QCD}'}^2 r, \tag{2.15}$$

where c is an order one number obtained from non-perturbative physics. For the Coulomb term to dominate we need

$$\Lambda_{\text{QCD}'}^2 \ll \frac{2}{3}\alpha_s'(\mu)\mu^2. \tag{2.16}$$

To remain in the regime of perturbativity we also require $\alpha_s'(\mu) < 0.5$. In Fig. 1 we plot contours of the Δ' mass as a function of the twin top-quark mass $m_{t'}$ and the ratio of the twin bottom-quark Yukawa to the SM value. In the plot we choose the UV cutoff Λ_{UV} to be 5 TeV and take

$$\frac{g_3'(\Lambda_{\text{UV}}) - g_3(\Lambda_{\text{UV}})}{g_3(\Lambda_{\text{UV}})} \equiv \delta g_3' = -0.15, \tag{2.17}$$
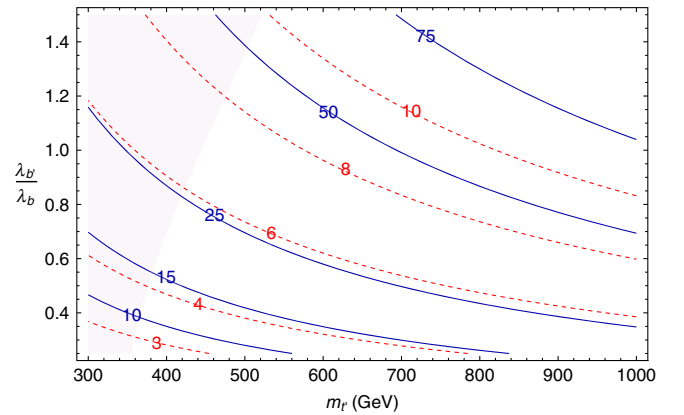

FIG. 1. Contours of the Δ' baryon mass in GeV (solid blue) and the ratio $\mu/\Lambda_{\text{QCD}'}$ (dashed red) as a function of $m_{t'}$ and the ratio of the twin bottom Yukawa to the SM value. The definition of μ is given in Eq. (2.14). The shaded purple area is in tension with Higgs coupling measurements.

to ensure we remain within the perturbative regime over the entire parameter space. As the figure makes clear, the baryon masses that best match a naive realization of ADM, that is with $m_{\rm DM} \sim 5m_N$, occur for smaller $\lambda_{b'}$ and smaller $m_{t'}$. We also note that if the bottom Yukawa is reduced too much, we violate (2.16). We avoid these situations by taking $\lambda_{b'}/\lambda_b > 0.15$. The dashed red lines of the figure indicate contours of $\mu/\Lambda_{\rm QCD'}$, which control the size of corrections to our numerical calculation.

The figure also shades in the area in tension with Higgs coupling measurements. These regions of the parameter space reduce the rates of Higgs production and decay into visible states below 80% of the SM prediction, which is the current bound; see Refs. [19,30,52]. Therefore we find that the allowed range of twin baryon masses is about 10–100 GeV. Comparing this to the requirements of ADM in Eq. (1.1) we find that the twin baryon asymmetry $\eta_{\rm DM}$ needs to be between $\eta_{\rm B}/2$ and $\eta_{\rm B}/20$.

III. TWIN BARYON DARK MATTER

The spectrum of the fraternal twin sector is determined largely by the masses of the twin b' quark, τ', and τ' neutrino. While the framework accommodates many choices, we focus on twin masses close to their SM partners. That is, we assume both the b' and τ' to have masses of at least a few GeV, while the ν'_τ is much lighter. In this case the twin $W'^\pm$ decays quickly to the lighter leptons, which are stable.

The hadron spectrum is composed of $\bar{b}'b'$ mesons, $b'b'b'$ baryons, and glueballs. These last have masses set by the twin confinement scale, varying from $7\Lambda_{\rm QCD'}$ to $18\Lambda_{\rm QCD'}$. The glueballs and mesons decay quite rapidly through twin weak interactions into twin neutrinos and lighter glueball or meson states. A few of these states also mix with the Higgs, allowing for decays into SM final states. The lightest baryon state, the spin $3/2$ Δ' with mass $m_{\Delta'} \sim 3m_{b'}$, is stabilized by its nonzero twin baryon number.

In the fraternal twin Higgs setup the twin hypercharge may or may not be gauged. From pure $\Delta N_{\rm eff}$ considerations it is better to have no massless d.o.f. in the dark sector. In such a scenario the leptons are largely unimportant as far as DM signals go, and their dynamics and signals have been discussed elsewhere [46–48]. For the remainder of this section we turn to the constraints on the twin baryons as DM.

The self-scattering cross section of Δ' baryons can be estimated from their mutual long range van der Waals potential:

$$V_{\rm vdW}(r) \approx c_{\rm vdW} \frac{\alpha'_s}{\mu^5} \frac{1}{r^6}, \tag{3.1}$$

for few $\times \Lambda_{\rm QCD'} < r^{-1} < \mu$, where $c_{\rm vdW}$ is an order one number and μ is the characteristic momentum scale of the

quarks given in Eq. (2.14). For $r > \Lambda_{\rm QCD'}^{-1}$ there is no potential between two baryons since there are no light twin mesons to exchange. The cross section is then given by [57]

$$\sigma \approx \frac{9\pi}{4} \left(\frac{3\pi\alpha'_s c_{\rm vdW} m_{\Delta'}}{8\mu^5 k} \right)^{2/5}, \tag{3.2}$$

where $\mu > k > \Lambda_{\rm QCD'}$ is the momentum transfer. The scattering cross section for DM is bounded [58] to be less than

$$\frac{\sigma}{m_{\rm DM}} \lesssim 0.47 \frac{\rm cm^2}{\rm g} = (13 \; {\rm GeV}^{-1})^3, \tag{3.3}$$

for the DM to be consistent with observations, primarily that of the Bullet Cluster [2]. To obtain a conservative bound we take the smallest value of $k = \Lambda_{\rm QCD'}$ and the largest coupling value, $\alpha'_s = 0.5$ in the numerator. So the cross section bound is satisfied for sufficiently heavy b's:

$$\left(\frac{\mu^5 \Lambda_{\rm QCD'} m_{b'}^{3/2}}{c_{\rm vdW}} \right)^{2/15} \gtrsim 0.11 \; {\rm GeV}. \tag{3.4}$$

Going to the edge of the interesting parameter space, $m_{t'} = 300$ GeV, $\lambda_{b'}/\lambda_b = 0.15$, and taking a large van der Waals coefficient of $c_{\rm vdW} = 100$ gives[3] a value of 0.3 GeV for the left-hand side of (3.4), well above the bound. For larger $m_{t'}$ and $\lambda_{b'}$ the bound is even more easily satisfied.

Direct detection of twin baryon DM is dominated by Higgs exchange. This contrasts with [48] whose authors also needed to consider b' meson exchange, which can dominate in the strong coupling regime. With the b' masses above the confinement scale, however, the effective coupling between the baryon Δ' and the mesons is small and the mesons are heavy. Then, the leading effect is simply from t-channel Higgs exchange between a target nucleon and twin baryon.

We parametrize the coupling of the Higgs h to the nucleon N as

$$\frac{m_N}{v} f_N h\bar{N}N, \tag{3.5}$$

where f_N is calculated using lattice measurements of matrix elements of quark mass terms in the nucleon and their Yukawa couplings. In particular we use the definition

$$\langle N|m_q q\bar{q}|N\rangle \equiv m_N f_{T_q}^N. \tag{3.6}$$

For a coupling λ_q between the Higgs and the quarks, $\lambda_q hq\bar{q}$, the general Higgs coupling $F_N hN\bar{N}$ to the nucleon is

---

[3]In light atoms the analogous values of $c_{\rm vdW}$ range from 0.25 to 150.

$$F_N = \sum_q \frac{\lambda_q}{m_q} m_N f_{T_q}^N = \frac{m_N}{v} \sum_q \frac{m_q}{m_q} f_{T_q}^N \equiv \frac{m_N}{v} f_N. \quad (3.7)$$

Using the values in [59] we find $f_N \approx 0.3$. However, extraction of these parameters from recent experiments may point to slightly smaller values [60,61]; see also [62–64]. In this analysis we have neglected the $\sim v^2/f^2$ correction to the Higgs-quark couplings, which would slightly decrease the final cross section.

The coupling between the Higgs and the Δ' baryon is similarly defined,

$$\frac{m_{\Delta'}}{f} \frac{v}{f} f_{\Delta'} h \overline{\Delta'} \Delta', \quad (3.8)$$

to leading order in v/f. This leading factor of v/f comes from the Higgs coupling to the b', which is v/f suppressed relative to the SM coupling. Therefore, to leading order in v/f and the velocity of the DM the baryon-nucleon cross section is

$$\sigma_{N\Delta} \approx \frac{\mu_{N\Delta}^2}{\pi m_h^4} \frac{(f_N m_N)^2}{v^4} \frac{(f_{\Delta'} m_{\Delta'})^2}{(f/v)^4}, \quad (3.9)$$

where

$$\mu_{N\Delta} = \frac{m_N m_{\Delta'}}{m_N + m_{\Delta'}} \quad (3.10)$$

is the reduced mass of the nucleon-baryon system. Unlike the $m_{b'} \ll \Lambda_{\text{QCD}'}$ limit, we saw in Sec. II that the gluon contribution to $m_{\Delta'}$ is small. Thus, the coupling of the Higgs to the twin baryon is simply mediated by the coupling to the constituent quarks. Consequently, to leading order in α_s' we find $f_{\Delta'} = 1$.

This allows us to plot the direct detection sensitivity as a function of $m_{b'}$. In Fig. 2 we compare these sensitivities to the latest results from Xenon 1 Ton [65] for several values of the twin bottom-quark Yukawa coupling $\lambda_{b'}$. The experimental bounds are a function of the Δ' mass, which is itself a function of $m_{t'}$ and $\lambda_{b'}$. For each value of the Yukawa coupling we plot both the experimental bounds (solid line) and the projected signal (dashed line) as a function of the twin top-quark mass. We see that when the SM and twin Yukawas are equal only larger values of $m_{t'}$ are consistent with experiment. However, as the twin bottom Yukawa is decreased, the projected signal falls below the current bounds.

Recall from Fig. 1 that larger values of $m_{t'}$ also lead to larger $m_{\Delta'}$. In addition, it is clear that if $\lambda_{b'} > \lambda_b$ then even larger values of $m_{t'}$ and $m_{\Delta'}$ would be required to agree with experiment. Thus, direct detection and naturalness (preferring lighter $m_{t'}$) push us toward twin bottom Yukawas that are smaller than the SM value. This, in turn, reduces $m_{\Delta'}$, pushing it toward the naive ADM expectation of ~ 5 GeV.
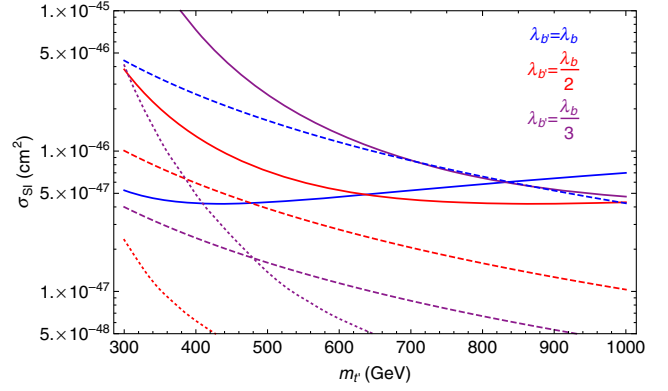

FIG. 2. Plot of the direct detection cross section (dashed) and experimental bounds (solid) as a function of the twin top-quark mass $m_{t'}$. Curves are shown for twin bottom Yukawa couplings equal to 1 (blue), 1/2 (red), and 1/3 (purple) times the SM value. Dotted lines correspond to the projected sensitivity of the LZ detector.

In short, the Δ' baryon is a successful ADM candidate, whose mass and scattering cross section can be determined with some precision. What is more, while the direct detection cross sections are smaller than the current limits, most are accessible to the proposed LUX-ZEPLIN (LZ) [66] experiment, whose projected sensitivities are given by the dotted lines in Fig. 2. Only the lightest mass states can escape detection there, but the high luminosity LHC run is expected to, at least indirectly, probe these states up to $m_{t'} = 500$ GeV through the corresponding modifications to Higgs couplings [30].

IV. TWIN ATOM DARK MATTER

If the twin $U(1)_{Y'}$ is gauged, then twin atoms composed of τ' particles bound to Δ's typically result. This is ensured by twin charge neutrality: the asymmetric production of Δ' requires a compensating asymmetry in τ'. The mass of the dark atom m_D is simply

$$m_D = m_{\Delta'} + m_{\tau'} - B_D, \quad (4.1)$$

where B_D is the binding energy, which is, to leading order,

$$B_D = \frac{\alpha'^2 \mu_D}{2}, \quad (4.2)$$

where μ_D is the reduced mass of the Δ'-τ' system and α' is the twin fine structure constant. Making use of the definition $R = m_{\Delta'}/m_{\tau'}$ we can then express the reduced mass (and therefore the binding energy) as

$$\mu_D \approx \frac{2 m_D R}{2(1+R)^2 - \alpha'^2 R}. \quad (4.3)$$

These relations are used repeatedly below.

If the recombination of these particles into twin atoms is not sufficiently efficient then the DM remains primarily a plasma, which can develop instabilities that affect galaxy collisions, like the Bullet Cluster [2]. This translates into a bound on the twin fine structure constant α' as a function of m_D [67]:

$$\frac{\alpha'^4}{\xi} \left(\frac{\Omega_D h^2}{0.11}\right) \left(\frac{\text{GeV}}{m_D}\right)^2 \left[\frac{(1+R)^2}{R} - \frac{1}{2}\alpha'^2\right]^2 \gtrsim 7.5 \times 10^{-11},$$

(4.4)

where $\Omega_D h^2$ is the relic density of dark matter and ξ is the ratio of the present day temperature of the dark radiation to the CMB temperature,

$$\xi = \left(\frac{T_D}{T_{\text{CMB}}}\right)\bigg|_{z=0}.$$

(4.5)

We determine ξ in steps. The Higgs portal keeps the two sectors in thermal equilibrium down to a decoupling temperature T_{dec} of a few GeV [37]. After decoupling the two sectors evolve independently, each conserving entropy. This allows us to relate the ratio of temperatures today ξ to the ratio at decoupling, which is $\xi_{\text{dec}} = 1$:

$$\xi = \xi_{\text{dec}} \left(\frac{g_*^{\text{today}} g_{*D}^{\text{dec}}}{g_*^{\text{dec}} g_{*D}^{\text{today}}}\right)^{1/3}.$$

(4.6)

Here $g_{*(D)}$ is the effective number of d.o.f. in the visible (dark) sector

$$g_* = \sum_{\text{bosons}} g_i + \frac{7}{8} \sum_{\text{fermions}} g_i,$$

(4.7)

where the sum is over all relativistic d.o.f. at a given temperature. For instance, at decoupling $g_*^{\text{dec}} = 75.75$ while $g_*^{\text{today}} = 3.94$ is the present value. If the two sectors decouple before the twin QCD phase transition, then g_{*D}^{dec} includes contributions from the twin gluons, making ξ much larger than otherwise. In other words, if the sectors decouple before the twin phase transition, then the twin photon and light leptons receive all the entropy from the phase transition, and their final temperature is correspondingly higher. By simply choosing $\delta g_3'$, as defined in Eq. (2.17), to be non-negative the twin confinement scale is $\gtrsim 5$ GeV [52], comfortably above the decoupling temperature.

The masses of the twin sector particles b', τ', and ν_τ' are not fixed, which affects the temperatures at which they are relativistic d.o.f. However, the b' is typically too heavy to contribute much at T_{dec}. Then, the largest value of ξ results from assuming that both the τ' and the ν_τ' contribute at decoupling, but neither do today. With these assumptions $\xi \approx 0.57$, which is well within the bounds on new

relativistic d.o.f. during big bang nucleosynthesis [67], but we must be more careful about the CMB bounds.

The energy density ρ at CMB times can be written as

$$\rho_{\text{CMB}} = \frac{\pi^2}{15} T_\gamma^4 \left[1 + \frac{7}{8}\left(\frac{4}{11}\right)^{4/3} N_{\text{eff}}^{\text{SM}} + \frac{7}{8}\left(\frac{4}{11}\right)^{4/3} \Delta N_{\text{eff}}\right],$$

(4.8)

where T_γ is the temperature of the visible photons. Assuming the twin τ' is nonrelativistic at these energies, and that the twin photon and twin neutrino ν_τ' have the same temperature, we obtain

$$\Delta N_{\text{eff}} = \xi_{\text{CMB}}^4 \left[\frac{8}{7}\left(\frac{11}{4}\right)^{4/3} + N_{\nu'}\right],$$

(4.9)

where $N_{\nu'}$ counts the number of active neutrino species at CMB energies. For $N_{\nu'} = 0$ we have $\xi \approx 0.57$ and $N_{\text{eff}} \approx 0.48$, in tension with the 2σ bound of $\Delta N_{\text{eff}} < 0.3$. However, if the twin neutrino is still active at CMB times then $\xi \approx 0.465$ and $N_{\text{eff}} \approx 0.25$ which agrees with current measurements. Thus, for the remaining bounds we take $\xi = 0.465$.

The bounds on the twin dark atom scenario from Eq. (4.4) are shown in Fig. 3 for three values of R. The figure makes clear that twin DM with lighter masses is less constrained. Also a larger mass hierarchy between $m_{\Delta'}$ and $m_{\tau'}$ weakens the constraint. If the twin QED coupling is similar to the SM value $\alpha' \lesssim 1/100$, then only lighter DM masses agree with the data.

A second bound on twin atoms comes from their self-interactions. Again, from [58] one finds that their self-interaction cross section must satisfy (3.3). The self-scattering cross section of twin atoms can be estimated from their mutual long range van der Waals potential:
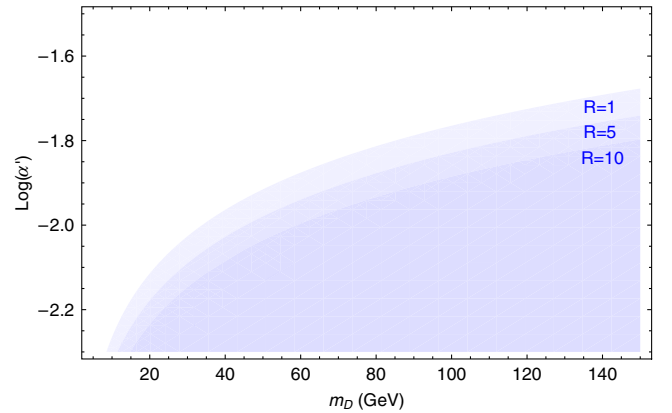

FIG. 3. Exclusion regions for dark atoms from dark plasma stability as a function of the dark atom mass m_D and the logarithm dark fine structure α'. Three benchmarks of $R = m_{\Delta'}/m_{\tau'}$ are shown.

$$V_{\text{vdW}}(r) \approx c_{\text{vdW,a}} \alpha' \frac{a^5}{r^6}, \qquad (4.10)$$

where $c_{\text{vdW,a}}$ is again an order one number and a is the twin Bohr radius,

$$a = \frac{1}{\alpha' \mu_D}. \qquad (4.11)$$

The cross section is then given by [57]

$$\sigma \approx \frac{9\pi}{4} \left(\frac{3\pi \alpha' c_{\text{vdW,a}} m_D a^5}{8k} \right)^{2/5}, \qquad (4.12)$$

where k is the momentum transfer.

It is possible that the velocity dependence of this cross section can solve a minor problem with standard DM candidates [54,55]. In order to make this comparison we use Eq. (4.12) to obtain

$$\frac{\sigma v_D}{m_D} \approx v_D^{3/5} \frac{9\pi}{16} \left(\frac{3\pi}{8} \right)^{2/5} C_D, \qquad (4.13)$$

where we have defined

$$C_D = \left(\frac{c_{\text{vdW,a}}}{\alpha'^4} \right)^{2/5} \frac{[2(1+R)^2 - \alpha'^2 R]^2}{m_D^3 R^2}. \qquad (4.14)$$

In Fig. 4 we plot this cross section as a function of velocity for several values of C_D in units of GeV^{-3}. Also shown are the data given in [54,55] obtained from dwarf and
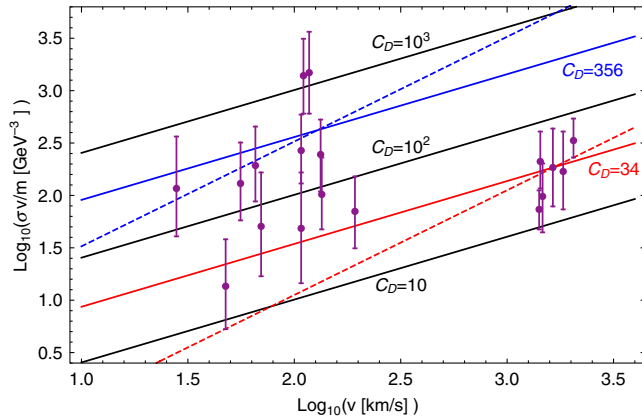

FIG. 4. Plot of the twin atom self-interaction cross section divided by DM mass and multiplied by velocity as a function of velocity for several values of C_D in units of GeV^{-3}. Data from dwarf galaxies and low surface brightness spiral galaxies are clustered at lower velocities with galaxy cluster measurements at higher velocities. In red (blue) we plot the best fit line appropriate to the galaxy cluster (galaxy only) data. These are compared to similar best fit lines corresponding to velocity independent cross sections.

low-surface-brightness galaxies (at lower velocities) and galaxy clusters (at higher velocities).

The figure shows separate best fit values for the low and high velocity data, which are $C_D = 356$ GeV^{-3} and $C_D = 34$ GeV^{-3} respectively. These lines are contrasted with similar best fit lines for DM with a velocity independent cross section. Taking the high velocity data as somewhat more consistent, we see that twin atom DM provides a better agreement with the low velocity data than DM with velocity independent cross sections. A similar velocity dependence would arise in any composite dark matter model [68–71] that has long range dipole-dipole interactions as in Eq. (4.10).

We can also use the plot to determine how the physical parameters, rather than the combination in C_D, must be related. The best fit to all the experimental data is $C_D \sim 55$ GeV^{-3}. Assuming this value we relate the remaining parameters. Specifically, by specifying $c_{\text{vdW,a}}$ we can explore how α' and m_D determine R. We provide some benchmarks in Table I, which are taken near the boundary where $C_D = 55$ GeV^{-3} can be solved for $R > 1$. For instance, taking the naive ADM benchmark of $m_D = 5$ GeV and $c_{\text{vdW,a}} = 1$ we must take $\alpha' \sim 1/15$ to obtain a real positive R, and find $R = 1.4$. Increasing α leads to larger R values. Larger R values result from further increasing α'. On the other hand, for $\alpha' = 1/137$ and $c_{\text{vdW,a}} = 10$ we must take $m_D = 20$ GeV to find a physical value for R, in this case $R = 1.3$, with larger R resulting from larger m_D. However, increasing m_D leads to tension with the recombination bounds shown in Fig. 3.

The above analysis applies to elastic scattering of the twin atoms. However, it has been shown [72] that the hyperfine splitting of the ground state can lead to inelastic scattering. This provides additional velocity dependence to the DM scattering which can explain some of the questions about large-scale structure; see [41] for another application of these results in the twin Higgs framework. During inelastic collisions the atom is up-scattered into this excited hyperfine state, which then decays by emitting hidden photons. This process can be important when the kinetic energy of the dark atoms is similar to the splitting between the hyperfine states. To estimate this splitting we simply adapt the standard result for hydrogen hyperfine splitting to our case with a spin-3/2 "proton." The energy splitting between the spin-2 states and spin-1 states is

TABLE I. Benchmark points near the real, positive $R > 1$ threshold with $C_D = 55$ GeV^{-3}. R can be increased by increasing either α' or m_D.

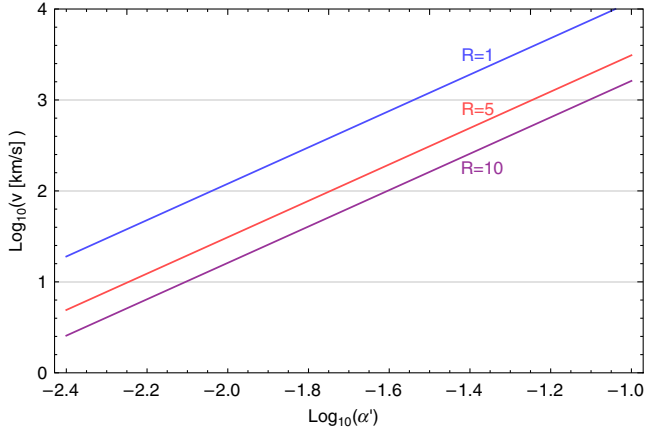| $c_{\text{vdW,a}}$	α'	m_D	R_{Min}
1	1/18	5 GeV	1.4
1	1/137	15 GeV	1.6
10	1/10	5 GeV	1.5
10	1/137	20 GeV	1.3

FIG. 5. Plot of the velocity when inelastic collisions to the hyperfine split excited ground state are maximized as a function of the twin fine structure constant for several values of R. We take $g_\Delta = 6$.

$$\Delta E_{\text{hf}} = \frac{8}{3} g_\Delta \alpha'^4 \frac{m_{\tau'}^2}{m_{\Delta'}} = \frac{8}{3} \frac{g_\Delta \alpha'^4 m_D (1 + R)}{R(1 + R)^2 - \alpha'^2 R^2 / 2}, \quad (4.15)$$

where g_Δ is the Landé g-factor of the Δ' and in the perturbative limit we are considering should be close to 6, the sum of the three $g_{b'}$'s. Note that this is a factor of 4 larger than the hydrogenlike case, because the twin baryon is spin-3/2. Then, by setting this equal to the kinetic energy $\frac{1}{2} m_D v^2$, we find the velocities v_{In} for which this type of scattering is important:

$$v_{\text{In}}^2 \sim \frac{16}{3} \frac{g_\Delta \alpha'^4 (1 + R)}{R(1 + R)^2 - \alpha'^2 R^2 / 2}. \quad (4.16)$$

In Fig. 5 we use Eq. (4.16) to find the velocities at which the inelastic collisions to the hyperfine excited state are most important. We see that there are parameter values where these collisions can further modify the velocity dependence of the self-scattering cross section. By comparing with Fig. 4 we note that as the ratio in particle masses R becomes larger the twin $U(1)$ coupling must become larger in order for the velocities associated with galaxy clusters to be affected. The typical velocities in the individual galaxy data can be modified when the twin coupling is closer to the SM value.

Before dark recombination the baryon-photon fluid in the twin sector undergoes acoustic oscillations. These can in turn leave traces on the visible matter power spectrum, affecting large scale structure. A detailed study of such dark acoustic oscillations [73] encapsulates these effects through the parameter Σ_{DAO}. In our case we estimate this quantity to be

$$\Sigma_{\text{DAO}} \approx \frac{2(1 + R)^2 - \alpha'^2 R}{\alpha' R} 10^{-9} \left(\frac{\text{GeV}}{m_D} \right)^{7/6}. \quad (4.17)$$

Since the constraints in Fig. 3 require $\alpha' \gtrsim 10^{-2}$, we find $\Sigma_{\text{DAO}} < 10^{-7}$, which is far below the sensitivity of current analyses.

Finally, the direct detection of these twin atoms is qualitatively similar to the baryon only case. There are additional Higgs exchange effects from the twin τ', but these are subleading to the baryon-baryon interactions, unless the twin τ' Yukawa coupling is raised considerably. In effect, this is controlled by R, since both the baryon and the τ' get much of their mass from the Higgs. So, for R somewhat larger than 1 the bounds in Fig. 2 should be approximately correct.

In short, twin atoms can make up an interesting ADM population. To have m_D values closest to 5 GeV, the τ' mass should be close to $m_{\Delta'}$, so that $R \sim 1$. These lightest mass atoms also require the α' coupling be somewhat stronger than in the visible sector. In addition, the velocity dependence of the self-interaction of these twin atoms agrees with self-interaction estimates better than DM with a velocity independent self-interaction cross section.

V. CONCLUSIONS

The fraternal twin Higgs scenario provides simple asymmetric DM candidates while stabilizing the Higgs mass up to TeV scales. We have demonstrated that twin baryons, whose constituent quarks have masses above the twin confining scale, successfully realize the ADM construction in a simple way. This is true both when the twin $U(1)$ is gauged and when it is not.

The most compelling regions of parameter space have lighter quarks and baryons, which also reduces the direct detection signal. Thus, the observation that $\Omega_D M \simeq 5\Omega_B$ is correlated with direct detection signals below the current state of the art. However, projected next generation sensitivities cover nearly all the motivated parameter space. The remaining parameter range will be indirectly probed by Higgs coupling measurements at the LHC. Other LHC searches, including for displaced vertices associated with boson decays, provide additional experimental tests of the fraternal twin Higgs setup. In the case of twin atoms, it would be interesting to work out how much clumping can occur as a result of inelastic scattering.

[1] V. C. Rubin, W. K. Ford, Jr., and N. Thonnard, Extended rotation curves of high-luminosity spiral galaxies. IV. Systematic dynamical properties, Sa through Sc, Astrophys. J. **225,** L107 (1978).

[2] D. Clowe, M. Bradac, A. H. Gonzalez, M. Markevitch, S. W. Randall, C. Jones, and D. Zaritsky, A direct empirical proof of the existence of dark matter, Astrophys. J. **648,** L109 (2006).

[3] D. B. Kaplan, A Single Explanation for Both the Baryon and Dark Matter Densities, Phys. Rev. Lett. **68,** 741 (1992).

[4] S. I. Blinnikov and M. Y. Khlopov, On possible effects of 'mirror' particles, Yad. Fiz. **36,** 809 (1982) [Sov. J. Nucl. Phys. **36,** 472 (1982)].

[5] E. D. Carlson and S. L. Glashow, Nucleosynthesis versus the mirror universe, Phys. Lett. **193B,** 168 (1987).

[6] R. Foot, H. Lew, and R. R. Volkas, A model with fundamental improper space-time symmetries, Phys. Lett. B **272,** 67 (1991).

[7] Z. Chacko, H. S. Goh, and R. Harnik, The Twin Higgs: Natural Electroweak Breaking from Mirror Symmetry, Phys. Rev. Lett. **96,** 231802 (2006).

[8] R. Barbieri, T. Gregoire, and L. J. Hall, Mirror world at the large hadron collider, arXiv:hep-ph/0509242.

[9] Z. Chacko, Y. Nomura, M. Papucci, and G. Perez, Natural little hierarchy from a partially Goldstone twin Higgs, J. High Energy Phys. 01 (2006) 126.

[10] G. Burdman, Z. Chacko, H. S. Goh, and R. Harnik, Folded supersymmetry and the LEP paradox, J. High Energy Phys. 02 (2007) 009.

[11] H. Cai, H. C. Cheng, and J. Terning, A quirky little Higgs model, J. High Energy Phys. 05 (2009) 045.

[12] D. Poland and J. Thaler, The dark top, J. High Energy Phys. 11 (2008) 083.

[13] N. Craig, S. Knapen, and P. Longhi, Neutral Naturalness from Orbifold Higgs Models, Phys. Rev. Lett. **114,** 061803 (2015).

[14] B. Batell and M. McCullough, Neutrino masses from neutral top partners, Phys. Rev. D **92,** 073018 (2015).

[15] J. Serra and R. Torre, Neutral naturalness from the brother-Higgs model, Phys. Rev. D **97,** 035017 (2018).

[16] C. Csáki, T. Ma, and J. Shu, Trigonometric Parity for Composite Higgs Models, Phys. Rev. Lett. **121,** 231801 (2018).

[17] T. Cohen, N. Craig, G. F. Giudice, and M. Mccullough, The hyperbolic Higgs, J. High Energy Phys. 05 (2018) 091.

[18] H. C. Cheng, L. Li, E. Salvioni, and C. B. Verhaaren, Singlet scalar top partners from accidental supersymmetry, J. High Energy Phys. 05 (2018) 057.

[19] G. Burdman, Z. Chacko, R. Harnik, L. de Lima, and C. B. Verhaaren, Colorless top partners, a 125 GeV Higgs, and the limits on naturalness, Phys. Rev. D **91,** 055007 (2015).

[20] D. Buttazzo, F. Sala, and A. Tesi, Singlet-like Higgs bosons at present and future colliders, J. High Energy Phys. 11 (2015) 158.

[21] D. Curtin and C. B. Verhaaren, Discovering uncolored naturalness in exotic Higgs decays, J. High Energy Phys. 12 (2015) 072.

[22] D. Curtin and P. Saraswat, Towards a no-lose theorem for naturalness, Phys. Rev. D **93,** 055044 (2016).

[23] H. C. Cheng, S. Jung, E. Salvioni, and Y. Tsai, Exotic quarks in twin Higgs models, J. High Energy Phys. 03 (2016) 074.

[24] H. C. Cheng, E. Salvioni, and Y. Tsai, Exotic electroweak signals in the twin Higgs model, Phys. Rev. D **95,** 115035 (2017).

[25] R. Contino, D. Greco, R. Mahbubani, R. Rattazzi, and R. Torre, Precision tests and fine tuning in twin Higgs models, Phys. Rev. D **96,** 095036 (2017).

[26] A. Ahmed, Heavy Higgs of the twin Higgs models, J. High Energy Phys. 02 (2018) 048.

[27] Z. Chacko, C. Kilic, S. Najjari, and C. B. Verhaaren, Testing the scalar sector of the twin Higgs model at colliders, Phys. Rev. D **97,** 055031 (2018).

[28] D. Buttazzo, D. Redigolo, F. Sala, and A. Tesi, Fusing vectors into scalars at high energy lepton colliders, J. High Energy Phys. 11 (2018) 144.

[29] F. Bishara and C. B. Verhaaren, Singleton portals to the twin sector, arXiv:1811.05977.

[30] C. Kilic, S. Najjari, and C. B. Verhaaren, Discovering the twin Higgs boson with displaced decays, Phys. Rev. D **99,** 075029 (2019).

[31] S. Alipour-Fard, N. Craig, S. Gori, S. Koren, and D. Redigolo, The second Higgs at the lifetime frontier, arXiv:1812.09315.

[32] Y. Bai, R. Lu, S. Lu, J. Salvado, and B. A. Stefanek, Three twin neutrinos: Evidence from LSND and MiniBooNE, Phys. Rev. D **93,** 073004 (2016).

[33] C. Csaki, M. Geller, O. Telem, and A. Weiler, The flavor of the composite twin Higgs, J. High Energy Phys. 09 (2016) 146.

[34] R. Barbieri, L. J. Hall, and K. Harigaya, Effective theory of flavor for minimal mirror twin Higgs, J. High Energy Phys. 10 (2017) 015.

[35] N. Aghanim et al. (Planck Collaboration), Planck 2018 results. VI. Cosmological parameters, arXiv:1807.06209.

[36] R. Barbieri, L. J. Hall, and K. Harigaya, Minimal mirror twin Higgs, J. High Energy Phys. 11 (2016) 172.

[37] Z. Chacko, N. Craig, P. J. Fox, and R. Harnik, Cosmology in mirror twin Higgs and neutrino masses, J. High Energy Phys. 07 (2017) 023.

[38] N. Craig, S. Koren, and T. Trott, Cosmological signals of a mirror twin Higgs, J. High Energy Phys. 05 (2017) 038.

[39] C. Csaki, E. Kuflik, and S. Lombardo, Viable twin cosmology from neutrino mixing, Phys. Rev. D **96,** 055013 (2017).

[40] M. Freytsis, S. Knapen, D. J. Robinson, and Y. Tsai, Gamma-rays from dark showers with twin Higgs models, J. High Energy Phys. 05 (2016) 018.

[41] V. Prilepina and Y. Tsai, Reconciling large and small-scale structure in twin Higgs models, J. High Energy Phys. 09 (2017) 033.

[42] Z. Chacko, D. Curtin, M. Geller, and Y. Tsai, Cosmological signatures of a mirror twin higgs, J. High Energy Phys. 09 (2018) 163.

[43] K. Fujikura, K. Kamada, Y. Nakai, and M. Yamaguchi, Phase transitions in twin Higgs models, J. High Energy Phys. 12 (2018) 018.

[44] L. Li and Y. Tsai, Detector-size upper bounds on dark hadron lifetime from cosmology, arXiv:1901.09936.

[45] M. Farina, A. Monteux, and C. S. Shin, Twin mechanism for baryon and dark matter asymmetries, Phys. Rev. D **94,** 035017 (2016).

[46] I. Garcia Garcia, R. Lasenby, and J. March-Russell, Twin Higgs WIMP dark matter, Phys. Rev. D **92,** 055034 (2015).

[47] N. Craig and A. Katz, The fraternal WIMP miracle, J. Cosmol. Astropart. Phys. 10 (2015) 054.

[48] I. Garcia Garcia, R. Lasenby, and J. March-Russell, Twin Higgs Asymmetric Dark Matter, Phys. Rev. Lett. **115,** 121801 (2015).

[49] M. Farina, Asymmetric twin dark matter, J. Cosmol. Astropart. Phys. 11 (2015) 017.

[50] Y. Hochberg, E. Kuflik, and H. Murayama, Twin Higgs model with strongly interacting massive particle dark matter, Phys. Rev. D **99,** 015005 (2019).

[51] H. C. Cheng, L. Li, and R. Zheng, Coscattering/coannihilation dark matter in a fraternal twin Higgs model, J. High Energy Phys. 09 (2018) 098.

[52] N. Craig, A. Katz, M. Strassler, and R. Sundrum, Naturalness in the dark at the LHC, J. High Energy Phys. 07 (2015) 105.

[53] N. Craig, S. Knapen, P. Longhi, and M. Strassler, The vector-like twin Higgs, J. High Energy Phys. 07 (2016) 002.

[54] X. Chu, C. Garcia-Cely, and H. Murayama, Puffy dark matter, arXiv:1901.00075.

[55] M. Kaplinghat, S. Tulin, and H. B. Yu, Dark Matter Halos as Particle Colliders: Unified Solution to Small-Scale Structure Puzzles from Dwarfs to Clusters, Phys. Rev. Lett. **116,** 041302 (2016).

[56] K. Varga and Y. Suzuki, Precise solution of few body problems with stochastic variational method on correlated Gaussian basis, Phys. Rev. C **52,** 2885 (1995).

[57] H. S. W. Massey and C. B. O. Mohr, Free paths and transport phenomena in gases and the quantum theory of collisions. II.—The determination of the laws of force between atoms and molecules, Proc. R. Soc. Ser. A **144,** 188 (1934); H. S. W. Massey, Collisions between atoms and molecules at ordinary temperatures, Rep. Prog. Phys. **12,** 248 (1949).

[58] D. Harvey, R. Massey, T. Kitching, A. Taylor, and E. Tittley, The non-gravitational interactions of dark matter in colliding galaxy clusters, Science **347,** 1462 (2015).

[59] J. Ellis, N. Nagata, and K. A. Olive, Uncertainties in WIMP dark matter scattering revisited, Eur. Phys. J. C **78,** 569 (2018).

[60] J. M. Alarcon, J. Martin Camalich, and J. A. Oller, The chiral representation of the πN scattering amplitude and the pion-nucleon sigma term, Phys. Rev. D **85,** 051503 (2012).

[61] J. M. Alarcon, L. S. Geng, J. Martin Camalich, and J. A. Oller, The strangeness content of the nucleon from effective field theory and phenomenology, Phys. Lett. B **730,** 342 (2014).

[62] J. Giedt, A. W. Thomas, and R. D. Young, Dark Matter, the CMSSM and Lattice QCD, Phys. Rev. Lett. **103,** 201802 (2009).

[63] I. Low, P. Schwaller, G. Shaughnessy, and C. E. M. Wagner, The dark side of the Higgs boson, Phys. Rev. D **85,** 015009 (2012).

[64] A. Crivellin, M. Hoferichter, and M. Procura, Accurate evaluation of hadronic uncertainties in spin-independent WIMP-nucleon scattering: Disentangling two- and three-flavor effects, Phys. Rev. D **89,** 054021 (2014).

[65] E. Aprile *et al.* (XENON Collaboration), Dark Matter Search Results from a One Ton-Year Exposure of XENON1T, Phys. Rev. Lett. **121,** 111302 (2018).

[66] D. S. Akerib *et al.* (LUX-ZEPLIN Collaboration), Projected WIMP sensitivity of the LUX-ZEPLIN (LZ) dark matter experiment, arXiv:1802.06039.

[67] F. Y. Cyr-Racine and K. Sigurdson, Cosmology of atomic dark matter, Phys. Rev. D **87,** 103515 (2013).

[68] D. S. M. Alves, S. R. Behbahani, P. Schuster, and J. G. Wacker, Composite inelastic dark matter, Phys. Lett. B **692,** 323 (2010).

[69] G. D. Kribs, T. S. Roy, J. Terning, and K. M. Zurek, Quirky composite dark matter, Phys. Rev. D **81,** 095001 (2010).

[70] M. Frigerio, A. Pomarol, F. Riva, and A. Urbano, Composite scalar dark matter, J. High Energy Phys. 07 (2012) 015.

[71] M. B. Wise and Y. Zhang, Stable bound states of asymmetric dark matter, Phys. Rev. D **90,** 055030 (2014); Erratum, Phys. Rev. D **91,** 039907(E) (2015).

[72] K. K. Boddy, M. Kaplinghat, A. Kwa, and A. H. G. Peter, Hidden sector hydrogen as dark matter: Small-scale structure formation predictions and the importance of hyperfine interactions, Phys. Rev. D **94,** 123017 (2016).

[73] F. Y. Cyr-Racine, R. de Putter, A. Raccanelli, and K. Sigurdson, Constraints on large-scale dark acoustic oscillations from cosmology, Phys. Rev. D **89,** 063517 (2014).